

# Series-Parallel Association of FET's for High Gain and High Frequency Applications

Carlos Galup-Montoro, *Member, IEEE*, Márcio C. Schneider, *Member, IEEE*, and Itamar J. B. Loss

**Abstract**—This paper presents a simple approach in the design of composite field effect transistors with low output conductance. These transistors consist of the series association of two transistors, with the transistor connected to the drain terminal wider than the transistor connected to the source terminal. It is shown that this composite transistor has the same dc characteristics as a long-channel transistor of uniform width. A composite transistor has two main advantages over its “dc equivalent” transistor of uniform width: significant area savings and a higher cutoff frequency. The main application is low-voltage, high-frequency analog circuits. The proposed technique is particularly suited for analog design in gate arrays.

## I. INTRODUCTION

THE MOS technology has proved to be well-suited for the implementation of mixed analog-digital systems. The growing trend towards smaller feature sizes and, consequently, lower supply voltages, leads to new challenges in the design of analog VLSI circuits [1]. A basic problem to be solved is the design of high-gain single-stage amplifiers [2]. High-gain amplifiers are typically obtained using long-channel transistors and/or cascode structures [3]. However, the transistor cutoff frequency is inversely proportional to the square of the channel length [4]. This property restricts the long-channel solution to low frequency applications. On the other hand, cascoding transistors results in a loss in linear output swing for the amplifier [3].

In this paper we propose a structure that has been inspired by a 1984 paper by Riccò [12]. This structure consists of the series association of two transistors where the transistor connected to the drain terminal is wider than the transistor connected to the source terminal. This composite transistor has a transconductance-to-output conductance ratio as high as that of a long-channel transistor but a shorter “physical channel length.” Hence, the composite transistor has a cutoff frequency higher than the cutoff frequency of its dc equivalent long-channel transistor. Therefore, the design of high-frequency, low-voltage simple analog sections [5] can benefit from the high attainable dc gain and high cutoff frequency of composite transistors. Moreover, composite transistors can be used for gate array implementation of analog sections in combined analog-digital circuits [6]–[8]. Two decisive advantages of

composite transistors for gate array design are significant area savings and simple modeling.

This paper describes the electrical performance of composite transistors as well as a set of equations for design purposes. The dc characteristics of composite transistors for both the triode and saturation regions are presented in Section II. Their dynamic behavior is analyzed in Section III. Experimental results for various prototypes of composite transistors are presented in Section IV while the conclusions are stated in Section V.

## II. DC CHARACTERISTICS OF COMPOSITE MOS TRANSISTORS

In this section, we demonstrate the dc equivalence between series connected and single transistors. Consider the series association shown in Fig. 1, which will be called a composite transistor in the text that follows. The gate and bulk terminals are common to both transistors. The channel lengths  $L_S$  and  $L_D$  are equal to or longer than the minimum length provided by the technology. We assume the gates of transistors  $M_S$  and  $M_D$  have rectangular geometries. This assumption does not represent any serious practical limitation because the rectangular geometry is the prevalent in VLSI layouts.

### A. Triode Region

In the triode region, using the gradual channel approximation, the drain current of an MOS transistor can be written [4], [9] as:

$$I_D = \frac{W}{L} [g(V_G, V_S) - g(V_G, V_D)] \quad (1)$$

where all voltages are referred to the substrate, emphasizing the symmetry between drain and source.  $W$  and  $L$  are the channel width and channel length, respectively and  $g(V_G, V)$  is a function that describes the dc behavior of the MOS transistor, including body effect and mobility reduction. Secondary effects in the triode region such as drain-induced barrier lowering and velocity saturation [4], which can have some influence on the drain current, have not been included in the analysis that follows. Actually, the secondary effects do not necessarily have a significant influence in the triode region, as shown in the experimental section of this paper.

For the series connection of transistors (Fig. 1), assuming the drain voltage  $V_D$  is such that transistor  $M_D$  is biased in the triode region and the drain currents of  $M_S$  and  $M_D$  are

Manuscript received October 29, 1993; revised April 4, 1994. The Brazilian MPC was supported by the Centro Tecnológico para Informática.

The authors are with the Laboratório de Instrumentação Eletrônica—Departamento de Engenharia Elétrica, Universidade Federal de Santa Catarina—C. P. 476, 88 040 900, Florianópolis, SC, Brazil.  
IEEE Log Number 940414.

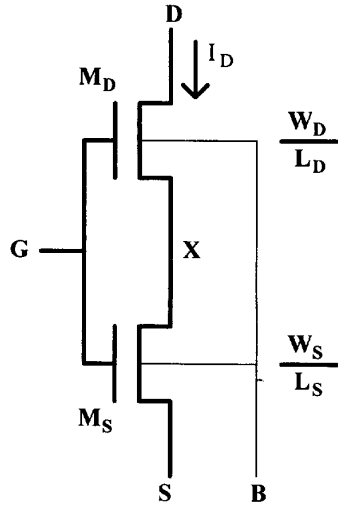


Fig. 1. Composite transistor.

equal, one obtains

$$g(V_G, V_X) = \frac{\left(\frac{W}{L}\right)_S g(V_G, V_S) + \left(\frac{W}{L}\right)_D g(V_G, V_D)}{\left(\frac{W}{L}\right)_S + \left(\frac{W}{L}\right)_D} \quad (2a)$$

from the application of (1) for both transistors. It should be pointed out that the value of function  $g(V_G, V_X)$  at the intermediate node  $X$  is the mean value of the values of  $g(V_G, V)$  at the source and drain terminals of the composite transistor. From (1) and (2a) the drain current in the composite transistor is

$$I_D = \left(\frac{W}{L}\right)_{eq} [g(V_G, V_S) - g(V_G, V_D)] \quad (2b)$$

where

$$\left(\frac{W}{L}\right)_{eq} = \frac{\left(\frac{W}{L}\right)_D \left(\frac{W}{L}\right)_S}{\left(\frac{W}{L}\right)_D + \left(\frac{W}{L}\right)_S} \quad (2c)$$

In the triode region, the composite transistor has a dc behavior equal to that of a single transistor whose aspect ratio is given by (2c). Hence, the geometric composition rule for the series connection of linear resistors (with the same sheet resistance) is also applicable to series-connected transistors [10].

On the verge of saturation the drain voltage is equal to the pinch-off voltage  $V_P$ , defined by the relation  $g(V_G, V_P) = 0$ . Obviously, the saturation voltage  $V_P$  is equal for transistors  $M_S, M_D$  and also for the series composition of  $M_S$  and  $M_D$ . Hence, (2a) and (2b) reduce to:

$$g(V_G, V_X) = \frac{g(V_G, V_S)}{1 + m} \quad (3a)$$

$$I_D = \frac{m}{1 + m} \left(\frac{W}{L}\right)_S g(V_G, V_S) \quad (3b)$$

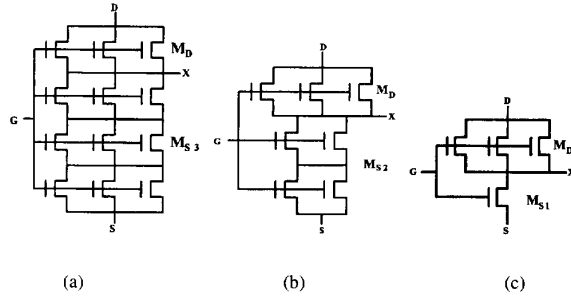


Fig. 2. Arrays of unit transistors with the same drain width ( $W_D = 3W_u$ ) and the same aspect ratio  $(W/L)_{eq} = 3/4$ . (a)  $(L/W)_{eq} = 3L_u/3W_u + L_u/3W_u$ , (b)  $(L/W)_{eq} = 2L_u/2W_u + L_u/3W_u$ , (c)  $(L/W)_{eq} = L_u/W_u + L_u/3W_u$ .

where  $m$  is the quotient of the aspect ratios

$$m = \frac{(W/L)_D}{(W/L)_S} \quad (3c)$$

From (3a), if  $M_S$  and  $M_D$  have equal channel lengths but  $M_D$  is much wider than  $M_S$ , then  $g(V_G, V_X)$  tends towards zero, i.e., the voltage at node  $X$  tends towards the pinch-off voltage. Hence, the aspect ratio of the composite transistor equals  $(W/L)_S$  and the current density in transistor  $M_D$  is much lower than in transistor  $M_S$ .

Obviously, the results of this section can be extended to a series association of any number of transistors and to the association of unit transistors in a rectangular array such as the one shown in Fig. 2(a). The aspect ratio of this type of array is equal to the aspect ratio of the unit transistor multiplied by the number of parallel-connected transistor and divided by the number of series-connected transistors. Transistors  $M_S$  and  $M_D$  (Fig. 1) of different widths and lengths can be implemented with rectangular arrays, as shown in Fig. 2. Arrays of unit transistors are useful either for gate array design [6]–[8] or in precision analog circuits [2].

### B. Saturation Region

In this section we demonstrate that the equivalence of any composite transistors in the triode region is extended to the saturation region if the composite transistors have, in addition to the same aspect ratio, the same channel width at the drain end. These two conditions are fulfilled by the composite transistors illustrated in Fig. 2. In these arrays, transistor  $M_D$ , identical for the three structures, is the transistor connected between nodes  $X$  and  $D$ . Transistors  $M_{S1}, M_{S2}$  and  $M_{S3}$ , connected between nodes  $X$  and  $S$ , have the same aspect ratio but different channel lengths.

The behavior of these composite transistors in saturation can be better understood with the aid of Fig. 3, which presents the classical determination of the operating point [11] from the output characteristics of transistors  $M_{S1}, M_{S2}, M_{S3}$  and from the load curve that represents transistor  $M_D$ . The difference in the two load curves shows that transistor  $M_D$ , which operates in the saturation region, presents a high output conductance. The near coincidence of the output characteristics of  $M_{S1}, M_{S2}$ , and  $M_{S3}$  in the triode region indicates, that

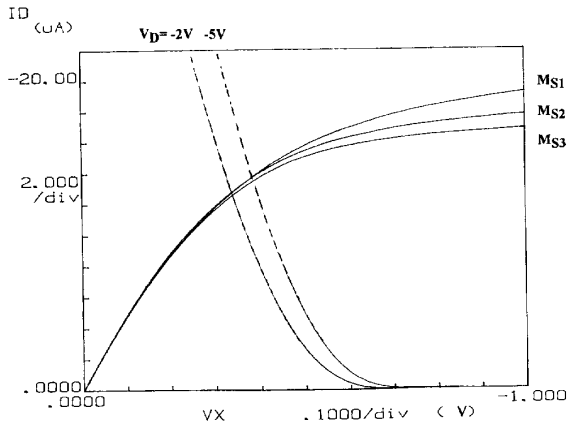


Fig. 3. Output characteristics of transistors  $M_{S1}$ ,  $M_{S2}$ ,  $M_{S3}$  and load curve due to transistor  $M_D$  from Fig. 2 at  $V_G = -1.8$  V.

transistors with the same aspect ratio have the same dc characteristics in this region despite the existence of short-channel effects. As expected, the operating point for the  $M_S$  transistors is in the triode region even if  $M_D$  is in the saturation region. Hence, the drain currents of the composite transistors of Fig. 2 in saturation and, consequently, their output conductances are approximately equal. Even though these conclusions have been reached through the analysis of an example, it should be clear that they can be extended to any composite transistors satisfying the trivial geometrical constraints enunciated at the beginning of this section.

For simplicity, we name two (composite) transistors as dc equivalent if they have the same dc current for the same bias. Generally, a composite transistor is not equivalent to itself if drain and source are interchanged [12]. Therefore, source and drain terminals should be physically identified.

Summarizing, any composite transistors with the same technological parameters are dc equivalent if they have:

- 1) the same aspect ratio,
- 2) the same channel width at the drain end, and
- 3) equal short-channel effects in the triode region (for both  $M_S$  and  $M_D$ ).

From conditions (i) and (ii), the "dc equivalent" electrical width and length of the composite transistor can be easily derived:

$$W_{eq} = W_D \quad (4a)$$

and from (2c) it follows that

$$L_{eq} = L_D + mL_S. \quad (4b)$$

Therefore, in order to obtain a composite transistor equivalent to a long-channel transistor, we should choose a transistor with  $m > 1$ , i.e., a composite transistor wider at the drain end than at the source end. The conventional way to obtain a low output conductance by means of a rectangular long-channel transistor reduces the electrical field along the whole transistor channel, giving rise to a long transit time, as shown in the next section. (4b) shows that a composite transistor

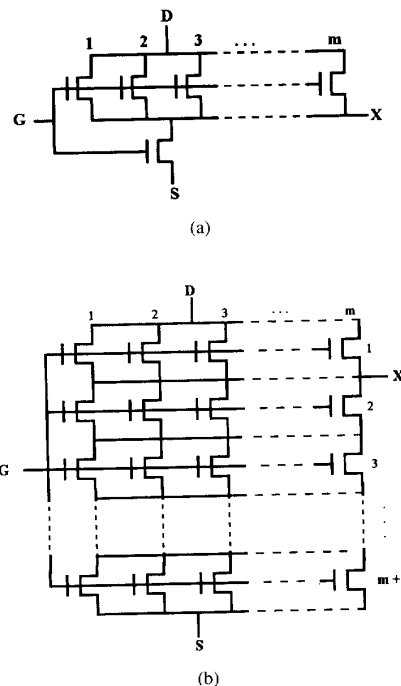


Fig. 4. Composite transistors: (a) Trapezoidal type composite transistor ( $T_m$ -transistor)  $(L/W)_{eq} = L_u/W_u + L_u/mW_u$ . (b) Rectangular type composite transistor ( $R_m$ -transistor)  $(L/W)_{eq} = mL_u/mW_u + L_u/mW_u$ .

equivalent to a long-channel transistor can be obtained from the series association of two minimum length transistors.

Fig. 4 shows an example of two dc equivalent arrangements of unit transistors. The trapezoidal transistor ( $T$ -transistor), whose drain end is wider than the source end, has the same aspect ratio and the same drain width as the rectangular transistor ( $R$ -transistor).

It should be noticed that the dc equivalence of transistors does not depend on the physical mechanisms of conduction provided the short-channel effects in the triode region are roughly the same (condition (iii)). This condition has been verified for transistors with minimum channel length in a 1.2- $\mu\text{m}$  standard CMOS process. Even if condition (iii) is not satisfied, the composite transistor wider at the drain end has a low output conductance in saturation due to the lower current density at the drain side.

### III. TRANSIT TIME

In this section we include an analysis concerning the dynamic behavior of the MOS composite transistor.

Usually, the transistor response to dynamic signals is characterized by the transit time ( $\tau$ ) and/or the intrinsic cutoff frequency ( $\omega_T$ ). For the saturated MOS transistor in strong inversion these two parameters are related [4] by

$$\tau\omega_T = 2. \quad (5a)$$

We demonstrate in Appendix A that (5a) is also approximately valid for a composite transistor.

The transit time in an MOS transistor is given [4] by:

$$\tau = \frac{Q_I}{I_D} \quad (5b)$$

where  $Q_I$  is the total inversion charge.

Therefore, the transit time in a composite transistor is

$$\tau = \frac{Q_{IS} + Q_{ID}}{I_D} \quad (5c)$$

where  $Q_{IS}$  and  $Q_{ID}$  are the total inversion charges in the transistors connected to the source and drain terminals, respectively. We calculate the drain current for the MOS transistor in strong inversion using the expressions from [2], [14]:

$$g(V_G, V) = \frac{\mu C'_{ox}}{2} n [V_P(V_G) - V]^2 \quad (6a)$$

where

$$V_P(V_G) \cong \frac{V_G - V_{T0}}{n} \quad (6b)$$

$\mu$  is the carrier mobility in the channel,  $C'_{ox}$  the gate capacitance per unit area,  $n$  the slope factor, which allows modeling the body effect, and  $V_{T0}$  the gate threshold voltage for the channel at equilibrium. All voltages are referred to the bulk. From (3) and (6) we determine the voltage at node  $X$  and the drain current in saturation

$$V_P - V_X = \frac{V_P - V_S}{\sqrt{1+m}} \quad (7a)$$

$$I_D = \frac{\mu C'_{ox} m W_S}{2(1+m)L_S} n (V_P - V_S)^2. \quad (7b)$$

On the verge of saturation, the drain voltage is equal to the pinch-off voltage  $V_P$ . The inversion charges [2], [13] are

$$Q_{IS} = \frac{2}{3} W_S L_S n C'_{ox} \frac{(V_P - V_S)^3 - (V_P - V_X)^3}{(V_P - V_S)^2 - (V_P - V_X)^2} \quad (7c)$$

$$Q_{ID} = \frac{2}{3} W_D L_D n C'_{ox} (V_P - V_X). \quad (7d)$$

We compute the transit time in the saturation region from (5c) and (7). For the MOS device shown in Fig. 4(a), the transit time is

$$\tau = \tau_u \left\{ \left[ \left( 1 + \frac{1}{m} \right)^2 - \frac{\sqrt{1+m}}{m^2} \right] + \sqrt{1+m} \right\} \quad (8a)$$

$$\tau_u = \frac{4L_u^2}{3\mu(V_P - V_S)}. \quad (8b)$$

In the previous analysis we have assumed that the transistors connected to the source and drain terminals have the minimum channel length, equal to  $L_u$ , provided by the technology. In this case,  $m$  is the ratio  $W_D/W_S$  and  $\tau_u$  is the transit time of the minimum-length transistor. In (8a) the first term, between square brackets, represents the transit time of the transistor connected to the source terminal while the second term is associated to the transit time of the transistor connected to the drain terminal. For high values of  $m$ , (8a) becomes

$$\tau \cong \tau_u \{ 1 + \sqrt{1+m} \}. \quad (8c)$$

The increase in the transit time for increasing values of  $m$  is due to the reduction of the electrical field in the channel of

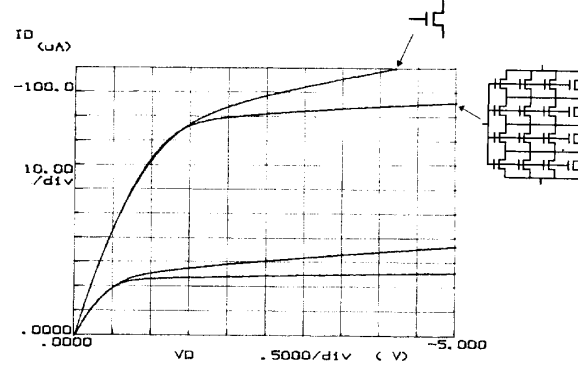


Fig. 5. Dc output characteristics of a unit transistor ( $W_u/L_u$ ) and of a square composite transistor ( $4W_u/4L_u$ ),  $L_u = 1.2 \mu\text{m}$ ,  $W_u = 3 \mu\text{m}$ .

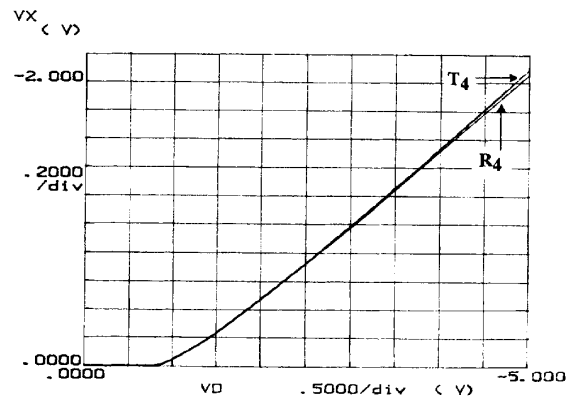
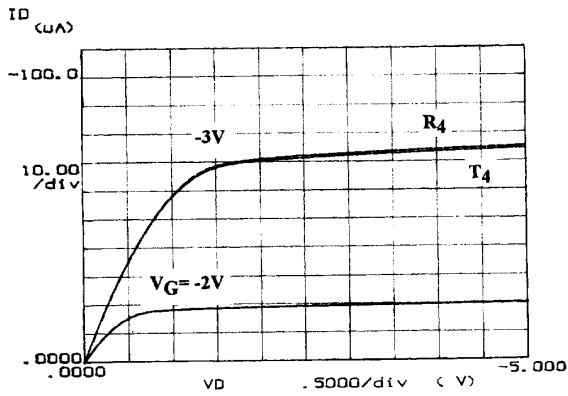


Fig. 6. Voltages at internal nodes  $X$  of the composite rectangular ( $R_4$ ) and trapezoidal ( $T_4$ ) transistors for  $V_D = V_G$ , with  $m$ , the number of parallel transistors at the drain side, equal to 4.

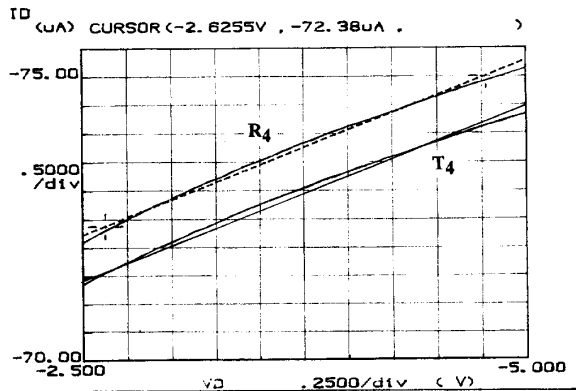
the composite transistor at the drain side. In fact, the electrical field at the channel of  $M_D$  decreases with the square-root of  $m$ , as can be inferred from (7a).

#### IV. EXPERIMENTAL RESULTS

In order to demonstrate the theoretical results, arrays of transistors of minimum channel-length in a  $1.2\text{-}\mu\text{m}$  CMOS n-well process ( $V_{TN} = 1.1 \text{ V}$ ,  $V_{TP} = -0.7 \text{ V}$ ) have been built. Fig. 5 shows the dc output characteristics of a single transistor and of a square array of transistors. Their equivalence in the triode region confirms that short-channel effects are negligible in this region. Indeed, the difference in the output conductances is evident. Fig. 6 displays the plots of the internal voltages  $V_X$  for the  $R$ -transistor and the  $T$ -transistor from Fig. 4, at  $V_D = V_G$ . Fig. 7 shows the output characteristics of the two arrays of transistors in Fig. 4. These characteristics are almost coincident, especially the output conductances in the saturation region. Hence, in spite of having a shorter physical channel, the  $T$ -transistor is dc equivalent to the  $R$ -transistor. The plots of the attainable low frequency gains ( $g_m/g_o$ ) for both p and n-channel integrated composite transistors are presented in Fig. 8. Voltage gains up to 60 dB are attainable with a



(a)



(b)

Fig. 7. (a) Dc characteristics of the composite rectangular ( $R_4$ ) and trapezoidal ( $T_4$ ) transistors. (b) Detail in the saturation region for  $V_G = -3$  V. The slopes of the straight lines represent the mean values of the output conductances.

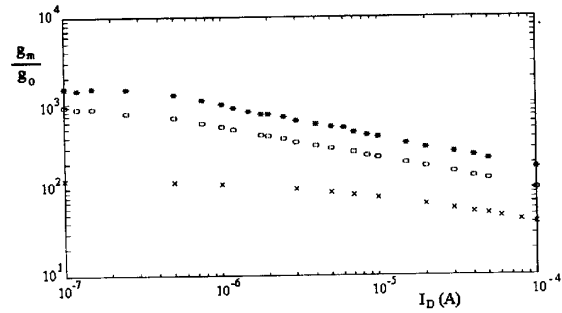
single stage of n-channel composite transistors, as shown in Fig. 8(a). Therefore, very high-gain amplifiers can be achieved by a single cascode stage of composite transistors.

As a means to verify experimentally the dependence of the transit time on the drain width (8a) we have written the normalized transit time (Appendix A) in strong inversion as:

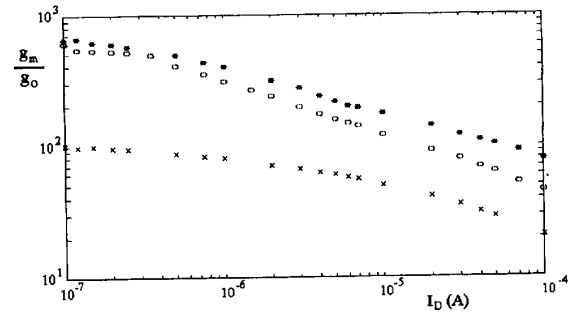
$$\frac{\tau}{\tau_u} = \frac{g_{mu} C_{gs}}{g_m C_{gsu}} \quad (9)$$

where  $C_{gs}(C_{gsu})$  and  $g_m(g_{mu})$  are the intrinsic gate-to-source capacitance and the small-signal gate transconductance of the composite (unit) transistor.

In order to measure the normalized transit time, we have built composite transistors with p-channel devices of the C4007 off-the-shelf circuit because of the very small capacitance of the available integrated transistors. We have determined the transit time for composite transistors that consist of a single transistor connected to the source end and  $m$  parallel-connected transistors to the drain side. The



(a)



(b)

Fig. 8. Attainable low frequency gain ( $g_m/g_o$ ) for the unit transistor ( $L_u = 1.2 \mu\text{m}$ ) and in composite transistors: x, unit transistor; o, trapezoidal transistor  $T_3$ ; \*, trapezoidal transistor  $T_5$ . (a) n-channel. (b) p-channel.

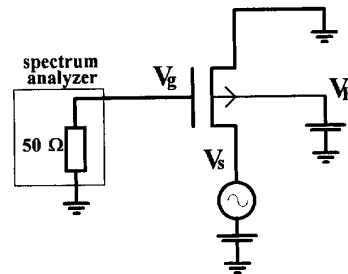


Fig. 9. Circuit to measure the gate-to-source capacitance.

values of the transconductances have been measured in a semiconductor parameter analyzer while the capacitances have been measured according to the scheme shown in Fig. 9. The experimental results obtained from the circuit in Fig. 9 for both a  $T$ -transistor and its dc equivalent uniform-width transistor are shown in Fig. 10. The capacitive coupling and, in consequence, the transit time in the  $R$ -transistor is about 6 times larger than in the  $T$ -transistor.

Fig. 11 exhibits the normalized transit time of the composite transistor in terms of  $m$ , the number of unit transistors connected to the drain terminal. The transit time depends weakly on  $m$ , in particular for low values of  $m$ . As an example of the usefulness of the composite transistor, let us compare some properties of the dc equivalent transistors  $T_9$  and  $R_9$ . The area of  $R_9$  is 9 times larger than the area of  $T_9$  and the transit

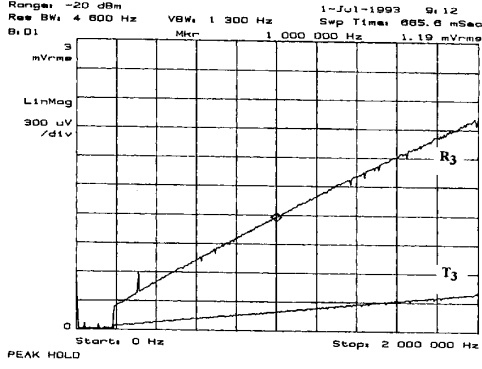


Fig. 10. Experimental results for the gate-to-source transadmittance in the rectangular ( $R_3$ ) and trapezoidal ( $T_3$ ) transistors  $V_{DB} = V_{GB} = -3\text{ V}$ ,  $V_{SB} = 0\text{ V}$ .

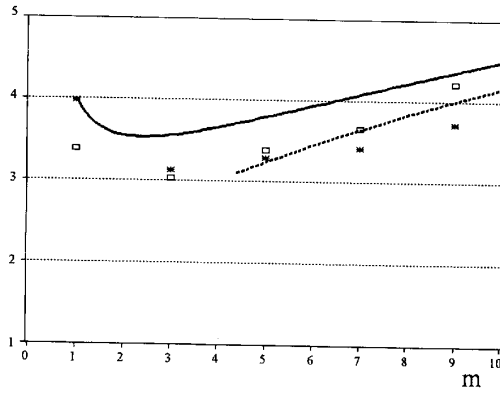


Fig. 11. Normalized transit time of the  $T_m$ -transistor ( $m$  is the number of parallel-connected transistors at the drain side): — theoretical; ---, asymptotic curve for high values of  $m$ ;  $\square$ , experimentally determined at  $V_{GS} = -2\text{ V}$ ; \*, experimentally determined at  $V_{GS} = -3\text{ V}$ .

time of  $R_9$  is roughly 25 times longer than the transit time of  $T_9$  (Fig. 11).

The transistors employed for the transit time determination have large overlap capacitances. However, the effect of these overlap capacitances on the total gate-to-source capacitance varies in almost the same proportion as the intrinsic gate-to-source capacitances, as shown in Appendix B. Hence, the ratio  $C_{gs}/C_{gsu}$  in (9) is little affected by the extrinsic overlap capacitances.

Up to now we have considered only the transit time to analyze the dynamic behavior of the composite transistor. However, the effects of the gate-to-drain overlap capacitance should be taken into account for a specific design. In fact, increasing the number of parallel-connected transistors at the drain end increases simultaneously the transit time and the capacitances related to the drain terminal.

## V. CONCLUSIONS

We have proposed a method to design composite transistors by the series-parallel association of single transistors.

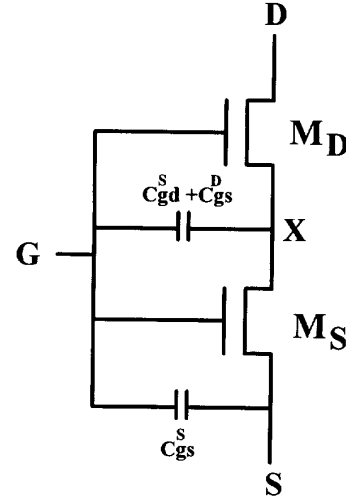


Fig. 12. Intrinsic capacitances in the composite transistor for the evaluation of the intrinsic gate-to-source capacitance.

The composite transistor has the high transconductance-to-output conductance ratio of a long-channel transistor with a reduced area and a higher cutoff frequency. Hence, composite transistors are very useful for the design of simple scheme analog sections for high-speed and low-voltage applications. Composite transistors also provide a natural solution for gate array design of analog circuits.

## VI. APPENDIX A

### Intrinsic Cutoff Frequency of the Composite Transistor

The gate-to-source capacitance  $C_{gs}$  is defined as [4], [13]:

$$C_{gs} = - \left. \frac{\partial Q_G}{\partial V_S} \right|_{V_G, V_D} \quad (\text{A1})$$

Using (A1) and the quasi-static operation approximation [4], the gate-to-source capacitance of the composite transistor (Fig. 12) can be written in terms of the gate capacitances of  $M_S$  and  $M_D$  as:

$$C_{gs} = C_{gs}^S + \frac{dV_X}{dV_S} (C_{gd}^S + C_{gs}^D) \quad (\text{A2})$$

where  $C_{gs}^S$  and  $C_{gd}^S$  are the gate-to-source and gate-to-drain capacitances of transistor  $M_S$  and  $C_{gs}^D$  is the gate-to-source capacitance of transistor  $M_D$ .

In strong inversion, the expressions for gate-to-source and gate-to-drain capacitances of a rectangular transistor are [13]:

$$C_{gs} = \frac{2}{3} C_{ox} \left[ 1 - \frac{(V_P - V_D)^2}{(2V_P - V_S - V_D)^2} \right] \quad (\text{A3})$$

$$C_{gd} = \frac{2}{3} C_{ox} \left[ 1 - \frac{(V_P - V_S)^2}{(2V_P - V_S - V_D)^2} \right] \quad (\text{A4})$$

where  $C_{ox} = C'_{ox} WL$ . We compute the gate-to-source capacitance  $C_{gs}$  of the composite transistor biased at saturation from (A2) to (A4) with  $V_X$  and its derivative with respect to

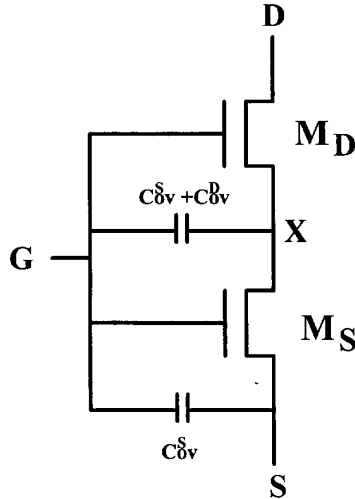


Fig. 13. Overlap capacitances in the composite transistor for the evaluation of the extrinsic gate-to-source capacitance.

$V_S$  determined from (7a). In the case of practical interest,  $L_S = L_D = L_u$ , the gate-to-source capacitance of the saturated composite transistor is given by

$$C_{gs} = \frac{2}{3} C'_{ox} W_S L_u \left[ 1 - \frac{1}{1+m} + \frac{1}{\sqrt{1+m}} \left( 1 + \frac{1}{\sqrt{1+m}} \right)^2 + \sqrt{1+m} \right]. \quad (A5)$$

The intrinsic cutoff frequency is calculated [4] from

$$\omega_T = \frac{g_m}{C_{gs} + C_{gb}} \cong \frac{g_m}{C_{gs}}. \quad (A6)$$

From (A5) and (A6), after some algebra, it follows that

$$\frac{1}{\omega_T} \cong \frac{C_{gs}}{g_m} = \frac{2L_u^2}{3\mu(V_P - V_S)} \cdot \left[ \left( 1 + \frac{1}{m} \right)^2 + \left( 1 - \frac{1}{m^2} \right) \sqrt{1+m} \right]. \quad (A7)$$

Therefore, (9) results from the comparison between (A7) and (8a).

## VII. APPENDIX B

### Effects of the Overlap Capacitances on the Gate-to-Source Capacitance of the Composite Transistor

Using the quasi-static operation approximation as in Appendix A, it follows (Fig. 13):

$$C_{ov} = C_{ov}^S + \frac{dV_X}{dV_S} (C_{ov}^S + C_{ov}^D) \quad (B1)$$

where  $C_{ov}$  is the equivalent extrinsic gate-to-source capacitance due to overlap capacitances  $C_{ov}^S$  and  $C_{ov}^D$  of transistors

$M_S$  and  $M_D$ . For  $L_S = L_D$ , it is readily verified that  $C_{ov}^D = mC_{ov}^S$ . Hence:

$$C_{ov} = C_{ov}^S (1 + \sqrt{1+m}). \quad (B2)$$

(B2) shows the same law for the extrinsic gate-to-source capacitance as that of the asymptotic behavior of the transit time for high values of  $m$  (8c).

## ACKNOWLEDGMENT

The authors would like to thank R. L. O. Pinto, G. Zolet, and A. L. Koerich for their help in measurements. The authors are greatly indebted to Dr. F. Krummenacher for very fruitful discussions.

## REFERENCES

- [1] P. E. Allen, "Future of analogue integrated circuit design," in *Analogue IC design: The Current-Mode Approach*, C. Toumazou, F. J. Lidgley and D. G. Haigh, Eds. London: Peter Peregrinus Ltd., 1990.
- [2] E. Vittoz, "MOS transistor," Intensive Summer Course on CMOS VLSI Design, Analog & Digital, Lausanne (EPFL), Switzerland, 1989.
- [3] P. J. Crowley, G. Roberts, "Designing operational transconductance amplifiers for low voltage operation," in *Proc. IEEE Int. Symp. on Circuits and Syst.*, Chicago, IL, May 1993, pp. 1455-1458.
- [4] Y. P. Tsividis, *Operation and Modeling of the MOS Transistor*. McGraw Hill, New York, 1987.
- [5] L. Moore, R. S. Soin, F. Maloberti, "Mixed analogue digital ASICs—circuit techniques, design tools and applications," Workshop on Analogue-Digital ASIC's, 5th Annual IEEE Int. ASIC Conf. and Exhibit, Rochester, NY, 1992.
- [6] S. Masuda *et al.*, "A CMOS analog and digital masterslice LSI," in *ISSCC Dig. Tech. Papers*, 1987, pp. 146-147.
- [7] P. Duchene and M. J. Declercq, "A highly flexible sea-of-gates structure for digital and analog applications," *IEEE J. Solid-State Circuits*, vol. 24, no. 3, pp. 576-584, June 1989.
- [8] S. Kawada *et al.*, "1.5- $\mu$ m CMOS gate arrays with analog/digital macros designed using common base arrays," *IEEE J. Solid-State Circuits*, vol. 24, no. 4, pp. 985-990, August 1989.
- [9] H. Wallinga and K. Bult, "Design and analysis of CMOS analog signal processing circuits by means of a graphical MOST model," *IEEE J. Solid-State Circuits*, vol. 24, no. 3, pp. 672-680, June 1989.
- [10] E. Vittoz and X. Arreguit, "Linear networks based on transistors," *Electron Lett.*, vol. 29, no. 3, pp. 297-299, Feb. 1993.
- [11] A. S. Sedra and K. C. Smith, *Microelectronic Circuits*, 2nd Ed. Fort Worth: Holt, Rinehart and Winston, 1987.
- [12] B. Ricc6, "Effect of channel geometries on FET output conductance in saturation," *IEEE Electron Device Lett.*, vol. 5, no. 9, pp. 353-356, Sept. 1984.
- [13] C. C. Enz, "High precision CMOS micropower amplifiers," Ph.D. thesis no. 802, EPF-Lausanne, Switzerland, 1989.
- [14] E. Vittoz, "Very low power circuit design: Fundamentals and limits," in *Proc. IEEE Int. Symp. Circuits and Syst.*, Chicago, IL, May 1993, pp. 1439-1442.



**Carlos Galup-Montoro** (M'89) was born in 1953 in Montevideo, Uruguay. He received the engineer degree in electronics from the Institut National Polytechnique de Grenoble (INPG), France, in 1979 and the doctor engineer degree in 1982, also from INPG.

From 1982 to 1989 he was at Universidade de São Paulo, São Paulo, Brazil, where he was involved in BIFET and CMOS analog design. Since 1990 he has been with the Electrical Engineering Department at Universidade Federal de Santa Catarina, Florianópolis, SC, Brazil, where he is now an Associate Professor. His current research interests are device modeling and integrated circuits design.



**Márcio Cherem Schneider** (M'90) was born in Florianópolis, SC, Brazil, in 1952. He received the B.E. and M.S. degrees in electrical engineering from the Universidade Federal de Santa Catarina (UFSC), Florianópolis, SC, Brazil, in 1975 and 1980, respectively. In 1984 he received the Doctoral degree in electrical engineering from the Universidade de São Paulo, São Paulo, Brazil.

Since 1976 he has been with the Electrical Engineering Department at UFSC, where he is now an Associate Professor. His research interests focus on semiconductor devices modeling and integrated circuits design.



**Itamar José Bassanezi Loss** was born in Mariópolis, PR, Brazil, in 1965. He received the B.E. and M.S. degrees in electrical engineering from the Universidade Federal de Santa Catarina (UFSC), Florianópolis, SC, Brazil, in 1988 and 1993, respectively.

From 1991 to 1993 he worked as a researcher at the Electronics Instrumentation Laboratory at UFSC. His current research interests focus on integrated circuits design.